



Electrokinetic Studies of Mine Tailings Considering Dewatering and Mass Transport at the Miduk Copper Mine, SE Iran

Foojan Shafaei^{1,2} · Faramarz Doulati Ardejani^{1,2} · Abbas Bahroudi¹ · Mohamad Yavarzade³ · Aliasghar Amini⁴

Received: 29 July 2020 / Accepted: 28 July 2021 / Published online: 2 August 2021
© Springer-Verlag GmbH Germany, part of Springer Nature 2021

Abstract

The effect of the electrokinetic process on the extraction of trapped water was evaluated in the Miduk copper mine's tailings slurry. The effect of the dewatering process on copper removal was also studied. The initial electroosmotic permeability was determined using a one-dimensional cell. In the next step, the effect of voltage and polarity reversal was evaluated for three scenarios: T1 (2 V/cm), T2 (2 V/cm), and T3 (1 V/cm). In addition, the polarity reversal method was applied to T2 and T3. To compare the amount of water extraction and energy consumption, three indices were considered and calculated: index of dry tone, water extraction, and normal water extraction. Moreover, the effect of electrokinetics on the final moisture content, physicochemical variation, and chemical composition were investigated. The results indicated that the calculated electroosmotic permeability ranged from 1.23×10^{-9} to 1.36×10^{-9} m²/V·S, which is acceptable for electrokinetic experiments. The water extraction experiments showed average flow rates of 1.68, 1.84, and 1.73 mL/h in T1, T2, and T3, respectively. The maximum amount of water extracted in T2 was $\approx 6\%$ more than in T3. However, considering electric energy consumption, the highest efficiency of water extraction was achieved by applying a voltage gradient of 1 V/cm for 24 h. Consequently, polarity reversal affected the water extraction efficiency by reducing energy consumption. Furthermore, moisture reduction due to the dewatering process decreased the pH variation and copper release and transport. Roughly 35% of the extractable copper was removed on the anode side of T2, which was determined to be the most efficient for remediation.

Keywords Water extraction · Energy consumption · Copper mine tailings · Electrochemical remediation

Introduction

Most mine tailings slurries contain a significant amount of processing water, which can be trapped for a long time in the tailings dam (Kossoff et al. 2014). The extraction and recovery of this trapped water can be essential in areas where there is a problem of providing water for mining activities. In addition, the presence of trapped water can affect the consolidation process and geotechnical parameters of accumulated tailings (Fourie and Jones 2010). Dewatering of mine tailings requires innovative approaches to reduce water consumption, facility costs, tailings dam footprints, and limit the risk of a tailings dam failure (Bourgès-gastaud et al. 2017; Huazhe et al. 2020).

There is a wide range of technologies to separate solid–liquid phases of mine tailings and industrial slurries. Sedimentation of dispersed fine-grained solids using aggregation, enhanced by coagulation-flocculation, is commonly used. However, in most cases, the flocs contain a significant amount of trapped water, especially between fine-grained

✉ Faramarz Doulati Ardejani
fdoulati@ut.ac.ir

Foojan Shafaei
f.shafaei@ut.ac.ir

Abbas Bahroudi
bahroudi@ut.ac.ir

Mohamad Yavarzade
yavarzadeh_m@nicico.com

Aliasghar Amini
aminialiasghar1364@gmail.com

¹ School of Mining, College of Engineering, University of Tehran, Tehran, Iran

² Mine Environment and Hydrogeology Research Laboratory (MEHR Lab), University of Tehran, PO Box: 1439957131, Tehran, Iran

³ Research and Development Center, National Iranian Copper Industries, Miduk Copper Mine, Kerman, Iran

⁴ National Iranian Copper Industries, Water Comprehensive Plan, Miduk Copper Mine, Kerman, Iran

particles due to the high amount of internal nano-scale capillaries (Huazhe et al. 2020; Wang et al. 2014). Accordingly, external energies must be applied to overcome this enormous capillary pressure, including mechanical, thermal, and electrical energies (Wang et al. 2014). Filtered materials often contain a high amount of trapped water after mechanical dewatering. Also, in some cases, a very high pressure is needed to reduce the water content of fine-grained materials (Ammami et al. 2020). Thermal technologies can do a better job dewatering and drying fine materials but consume more energy (Ammami et al. 2020; Mahmoud et al. 2010) and are inefficient at recovering and collecting the processing water. For in-situ applications, natural thermal drying can be used in arid and semi-arid regions. However, a large area is required to store the slurries in most cases and the optimal depth of natural drying is estimated at 0.5 m (Wang et al. 2014).

Electrokinetics is suitable for extracting and recovering trapped water, especially in fine-grained materials. In-situ application of electrokinetics is also used for the dewatering and remediation of ponds and settling areas (Dizon and Orazem 2020). Moreover, electrokinetic is a potential method for removal of contaminants, which is not the case of mechanical and thermal dewatering. Recently, many studies have been reported on the electrokinetic dewatering process for industrial sewage/sludge (Conrardy et al. 2016; Deng et al. 2020; Mahmoud et al. 2016; Wu et al. 2020), bio-solids (Navab-daneshmand et al. 2015; Zhang et al. 2017), geo-materials (Xue et al. 2019; Zhang and Hu 2019) and electrokinetic improvement of fine-grained and clayey soils (Abdullah and Al-Abadi 2010; Estabragh et al. 2014; Malekzadeh et al. 2016; Ou et al. 2009). Studies have been also performed in mining applications, such as Bourghès-Gastaud et al. (2017), Fourie and Jones (2010), Guo and Shang (2014), Lockhart (1983). Additionally, researchers have reported on the application of electrokinetics to remediate contaminated soils (Masi et al. 2017a, b; Rezaee et al. 2019; Rosestolato et al. 2015; Siyar et al. 2020) and to affect the fate and transport of potentially toxic elements in mine tailings (Hansen and Rojo 2007; Karaca et al. 2017; Oritz-Soto et al. 2019). Fourie et al. (2007) investigated the efficiency of electrokinetics as an in-situ technology for dewatering of very fine tailings, using a hexagonal arrangement of electrodes and applying a variable voltage gradient; water content was reduced from 158 to 75% in two months. The use of a dimensional stable anode (DSA) in the electro-dewatering of tailings slurry was reported by Lee et al. (2016), where polarity reversal improved the electroosmotic dewatering. However, their use of two water compartments as anode–cathode reservoirs saturated the media and therefore a true estimate of the amount of water content was not possible. Using a similar setup, Shang and Xu (2019) observed the

efficiency of electro-dewatering on nickel hydrometallurgical tailings, but did not consider energy consumption or the effects of dewatering on physicochemical variation and metal extraction.

In the current research, the effect of the electrokinetic process on the extraction of trapped water and metals were studied for mine tailings. Our main objectives were: investigating the efficiency of water extraction considering energy consumption; evaluating electric current variations in scheduling polarity reversals, as an enhancement method; investigating the effect of electrokinetic dewatering on moisture content reduction and physicochemical properties such as pH, electrical conductivity (EC), and resistivity; considering the effect of dewatering on the release and transport of copper; and investigating the potential of the method to be conducted in a pilot scale.

Materials and Methods

Study Area

The sample for laboratory experiments was obtained from the Miduk copper mine, located at 3,370,024 E and 324,133 N in UTM zone 40, in the Kerman province of Iran. It is one of the largest copper mines in Iran with about 171 million metric tons of copper and an average grade of 0.83% (Fig. 1). The main lithological units of the Miduk copper deposit include andesite, andesite-basalt, and volcano-clastic tuffs, as well as altered porphyritic diorites dikes and red sandstones as sedimentary units. The mineralisation occurred in the diorite porphyry rocks and the waste rocks often contain an andesite composition (Maghsoudy et al. 2019).

The Miduk complex includes the mining unit, concentrator plant, and a tailings structure. In the processing plant, the copper is extracted by adding collectors, frothers, depressants, activators, and modifiers to the crushed ore (Kargar et al. 2012). Due to a lack of water resources in the area, the tailings from the processing stage are directed to five thickeners for dewatering. By adding a conditioner, the recycled water is returned back to the processing plant. Finally, the slurry is directed to the channels with a total solids content of $\approx 60\%$ and enters into the tailings dam. Inside the tailings dam, the residual water content that accumulates in the tailings over time drain into an impoundment and is then pumped back to the plant. During this process, a considerable amount of water evaporates and leaves the cycle.

Principles of Electrokinetics in Soil

Applying an electric field to the soil triggers several physicochemical phenomena, which mostly include electrolysis of water molecules, electromigration, and electroosmosis. According to Helmholtz-Smolochowski's theory, the fluid flow rate per unit voltage gradient through a porous medium can be defined as electroosmotic permeability (m^2/sV):

$$k_{eo} = \frac{-\epsilon D}{\mu} n \quad (1)$$

In the above formula, D is the permittivity of pore fluid (F/m), μ denotes the fluid viscosity (Ns/m^2), n is the porosity of the media, and ϵ represents the zeta potential (mV). The most important parameter is the zeta potential of the particles, which is a function of the pH, the ionic strength of the fluid, and the mineralogy of the media (Acar and Alshawabkeh 1993; Reddy and Camesselle 2009). In experimental tests, the electroosmotic permeability is calculated using Eq. 2:

$$k_{eo} = \frac{Q_{eo}}{\nabla E \times A} \quad (2)$$

where Q_{eo} is the volumetric flow rate (m^3/s), ∇E is the gradient of electric potential (V/m), and A is the cross sectional area (m^2) of the soil (Reddy and Camesselle 2009).

Sampling and Preparation

Due to the swampy condition of the dam, it was not possible to survey all parts of it or take samples from most areas of the tailings dam. So, the experimental sample was taken from the inlet channel. To evaluate the suitable moisture content for performing the electrokinetic experiments, the moisture content of freshly accumulated tailings in five samples was measured and they averaged $\approx 33\%$. In the next step, 0.5 kg of slurry after homogenization was poured on a filter paper and sieve mesh no. 400 and allowed to drain for 24, 48, and 72 h to examine the ability of gravity to extract water. The average moisture content was almost 31%. Based on these results, it was decided to perform the electrokinetic experiments with 31% initial moisture content. For this purpose, tailings was collected from the inlet channel and dried at 105 °C for 24 h. After that, the tailings were homogenized and about 5 kg of soil was mixed with the processing water to reach 31% moisture content.

Properties of Tailings

Considering the physicochemical properties of the soil provides a better understanding of its behaviour during the

electrokinetic process. As shown in Table 1, pyrite (FeS_2) is the most common sulphide mineral in the Miduk mine tailings.

The D_{50} of the particles is equivalent to 0.054 mm and so the tailings can be classified as a fine-grained soil. The initial pH is alkaline due to the additives using in the processing stage. Also one of the important physicochemical properties of the soil particles is the surface charge. This charge depends on the pH of the liquid adjacent to the particles. At a certain pH, the surface charge and zeta potential are equal to zero, which is known as the point of zero charge (PZC). This pH value is important in electrokinetic studies, especially in reverse electroosmotic flow (Eq. 1). The PZC value of the tailings was measured as 4.2, following the approach presented by Cardenas-Peña et al. (2012).

Another important property of soils and tailings under electrokinetic process is buffering capacity, which indicates how the soil pH changes as a certain amount of acid or base is added to the soil media. The buffering of produced H^+/OH^- during electrokinetics can reduce the potential of release and even transport of the elements and can also weaken the effect of pH changes on the tailings' PZC and reduce the electroosmotic flow. The buffering capacity of the tailings (Fig. 2) was calculated by acid–base titration at a ratio of 1:2 (w-tailings/v-solution).

Experimental Setup and Procedure

In the first step, a one-dimensional cylindrical setup-box with a length of 24 cm and a radius of 8 cm, was utilised to evaluate the feasibility of using electrokinetics to enhance fluid flow through a tailings medium. The electroosmotic permeability of the saturated soil was also calculated. The electrodes were made of stainless-steel (SS316) and immersed inside the anode and cathode water compartments of the electrolyte. Figure 3a shows the schematic diagram of the experimental setups.

In the next step, a Plexiglas electrokinetic laboratory box $50 \times 20 \times 10$ ($\text{length}^{\text{cm}} \times \text{height}^{\text{cm}} \times \text{width}^{\text{cm}}$) were designed to evaluate the potential of electrokinetics for water extraction and moisture reduction without the anode and cathode water compartments (Fig. 3b). The stainless-steel electrodes (SS316) were inserted directly into the tailings. The main reason for using these types of electrodes was their availability and their relative low cost for both pilot and large-scale applications. Also, to reduce the evaporative effect, all setups were insulated with plastic nylon, and the laboratory temperature was maintained at 23 °C during the experiments.

To evaluate the potential of electrokinetics on the extraction of trapped water within the tailings, three experimental scenarios (T1, T2, and T3) were conducted (Table 2). During the experiments, the potential difference was kept constant

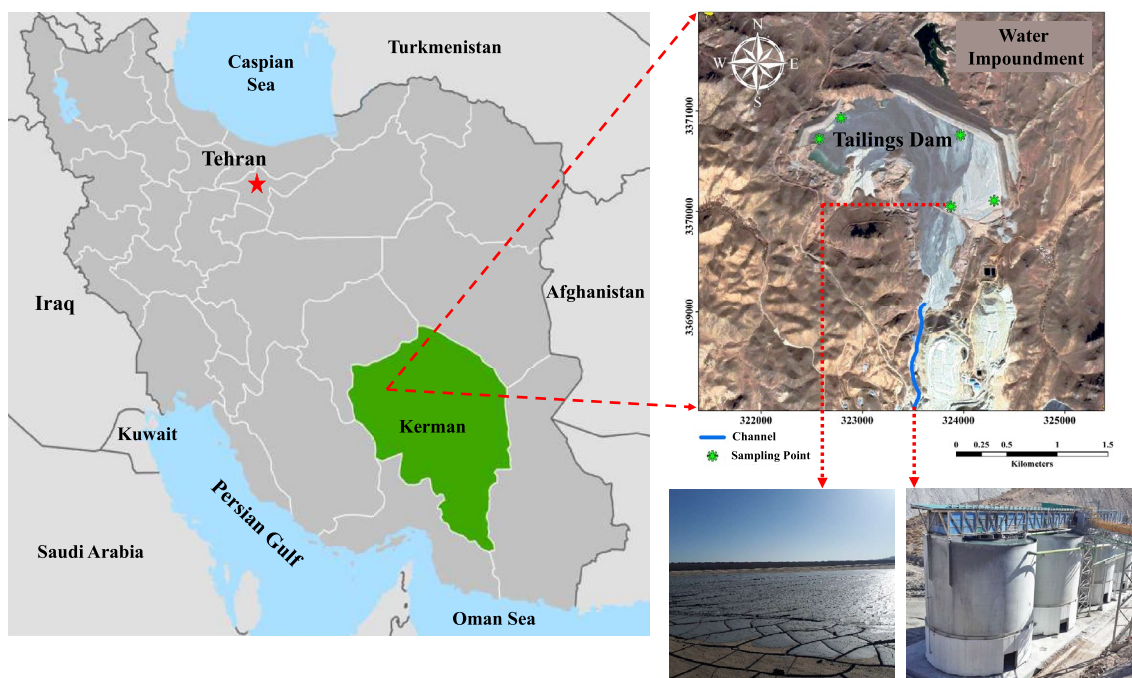


Fig. 1 Location map of Miduk copper mine, the tailings dam, the thickeners and sampling point

and the amount of electric current was recorded by a custom built data logger every 4 h.

After each experiment, the electrical resistivity of the tailings was measured by a cylindrical sample holder made of acrylic material (Fig. 3c). The dewatered tailings samples were taken from the anode, middle and cathode sections and then placed in the sample holder. To measure the electrical resistivity value four-electrode system of Wenner array was used.

Analytical Method

In the electrokinetic process, elements can be released from soluble phases to pore water due to the production and transportation of H^+ from the anode compartment, and then transported by electromigration and electroosmosis. The effect of electrokinetic dewatering on the geochemical composition of the dewatered tailings samples was investigated by a sequential extraction procedure. This method is based on the extraction of elements in different chemical fractions. To date, various techniques have been used to perform the sequential extraction procedure (Zimmerman and Weindorf 2010).

In the present study, the first phase included the separation of adsorbed metals on the soil surface called “exchangeable”. This phase represents the metals that can be easily separated from soil media and transported through the pores. Separation of this phase was done by changing the ionic

composition of a sample using a salt solution. All samples were prepared using a method presented by Maiz et al. (1997). Separation of this phase included agitation of the sample in 0.1 M solution of $CaCl_2$ for 2 h. The ratio was 1:10, w-soil/v-solution.

The acid-soluble fraction can be considered to check the amount of detachable elements during the electrokinetic process. Also, it shows the maximum ability to release and leach contaminants naturally due to the production of acidic drainage over time. The acid soluble fraction was determined by adding 5% sulphuric acid (v/v) to the tailings materials at a ratio of 1:10 w-soil/v-solution and stirring for 30 min. Finally, the filtered solution was diluted with 10 mL of concentrated HCl and distilled water to a volume of 100 mL (Ortiz-Soto et al. 2019).

In this study, the copper content in both the exchangeable and acid-soluble fractions are considered as part of the extractable phase. The chemical analysis of the residual fraction was performed using HNO_3 -HCl-HF (Maiz et al. 1997). Samples were sent to the laboratory to analyse the toxic elements by ICP-OES.

Electrokinetic Dewatering Efficiency

The electric energy consumption of each experiment was calculated by Eq. 3 (Ammami et al. 2020):

Table 1 Physicochemical characterisation of Miduk mine tailings

Major mineralogy					
Parameter	Value	Parameter	Value	Parameter	Value
Quartz	32%	Plagioclase	28.1%	Illite	22.7%
Alkali feldspar	12.3%	Pyrite	3.6%		
Physical parameters					
Parameter	Value	Parameter	Value	Parameter	Value
Zeta Potential (mV)	− 8	pH	8.3	Pore fluid EC (mS)	1.9
Resistivity (Ohm.m)	8.6	Liquid Limit (%)	25	D ₅₀ (mm)	0.054
Chemical composition-total concentrations of toxic metals(ppm)					
Parameter	Value (ppm)	Parameter	Value (ppm)	Parameter	Value (ppm)
Al	9838	Cu	418	V	47
Zn	42	Co	18	Cr	17
Ni	16	Pb	6		

$$E(kWh) = \int VI dt \quad (3)$$

In the above equation, V represents the voltage (V), I is the electric current (A), and E represents the energy consumption (kWh). The amount of energy consumption and extracted water are the most important factors in evaluating the economics of the dewatering process. Therefore, in order to compare the electrokinetic efficiency in dewatering, three indices were evaluated. The first index, which many researchers have described as the energy efficiency,

calculated the amount of energy consumption of the system per unit weight (tone) of dry tailings (IDT).

Due to the importance of the amount of extracted water, the consumed electric energy to extract one mL of trapped water was calculated as the index of water extraction (IWE):

$$IWE\left(\frac{kWh}{ml}\right) = \left(\frac{E}{W_w}\right) \quad (4)$$

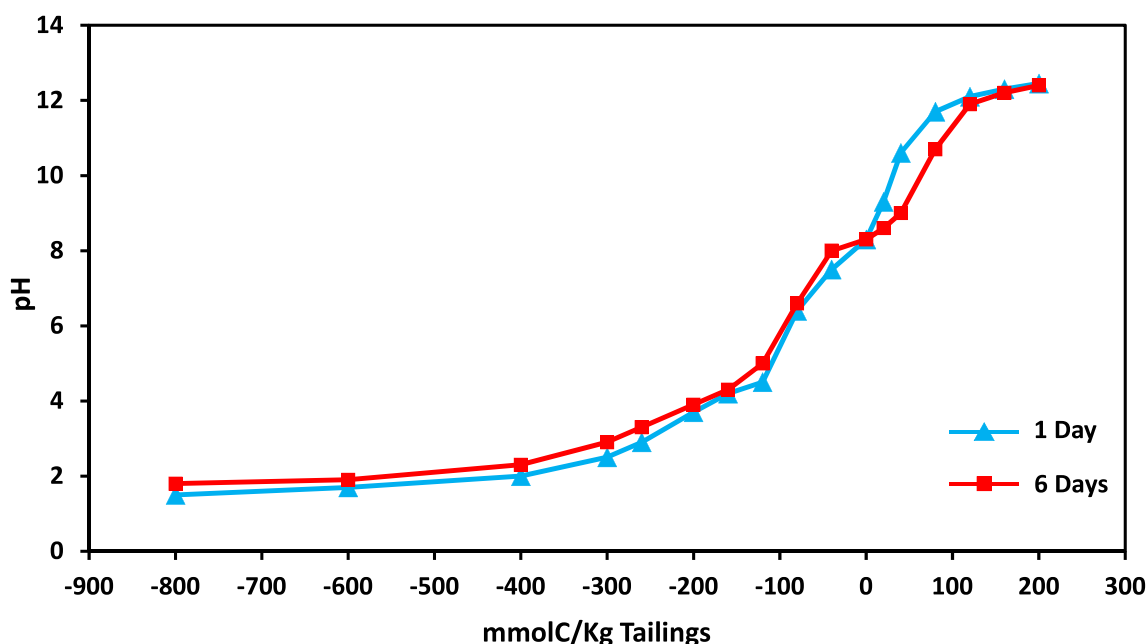


Fig. 2 Buffering capacity of the tailings materials

In this equation, W_w represents the extracted water (mL) and E represents the energy consumption (kWh), which was calculated using Eq. 3. However, the IWE index is not suitable for comparing the efficiency of the electrokinetic dewatering experiments for different weights of tailings. To solve this problem, the IDT and IWE were combined to form the index of normalized water extraction (INWE), which indicates the energy consumption for extracting one mL of water from a metric ton of dry tailings (Eq. 5):

$$INWE \left(\frac{kWh}{Dry-ton.mL} \right) = \left(\frac{E}{W_w \times W_T} \right) \quad (5)$$

In this formula, W_t is the dry ton of tailings (ton). Since the most optimal mode has less energy consumption and more water extraction, lower values of INWE are favourable. To achieve the most optimal time, the indices were also calculated for 3, 24, 48, 72, and 144 h in each experiment.

Table 2 Experimental scenarios for dewatering of the tailings

Experiment ID	Gradient voltage (V/Cm)	Polarity reversal	Electrodes (Anode and Cathode)	Operation time (h)
T1	2	No	SS316	144
T2	2	Yes	SS316	144
T3	1	Yes	SS316	144

Results and Discussion

Evaluation of Electroosmotic Permeability

Electroosmotic permeability is defined as the ability of the electric current to accelerate the fluid flow, which is specifically the fluid flow rate per unit of voltage gradient through a porous medium (Eq. 2). To evaluate the electroosmotic permeability of the tailings, the tailings sample was poured into a one-dimensional cylindrical system (Fig. 3a). In this system, the water level in the anode and cathode compartments was kept at the same level to ignore the effect of water flow due to the hydraulic gradient. Electroosmotic permeability was measured by applying voltage gradients of 1 and 2 V/cm. Each experiment was conducted for 24 h and the effluent

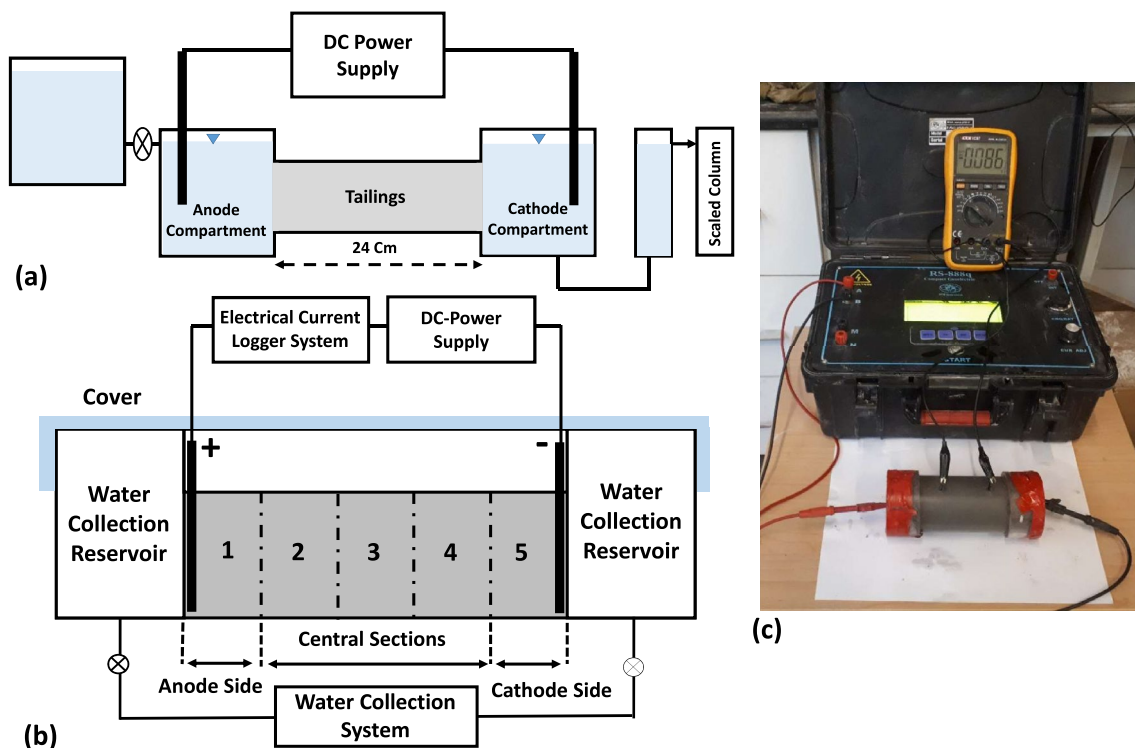


Fig. 3 Schematic diagram of experimental setups, 1D cylindrical setup-box for electroosmotic permeability measurement (a), electrokinetic setup box to evaluate extracted water and mass transport process (b), lab-scale geo-electrical system to measure electrical resistivity (c)

discharge from the cathode compartment was measured in the subsequent 4 and 24 h after starting each experiment. Electroosmotic permeability was achieved in the range of 1.23×10^{-9} to $1.36 \times 10^{-9} \text{ m}^2/\text{V}\cdot\text{S}$, which agrees well with previous studies, in which the range has been reported from 10^{-9} to $10^{-10} \text{ m}^2/\text{V}\cdot\text{S}$ for most clay soils and mine tailings (Chien et al. 2009; Lee et al. 2016; Masi et al. 2017a; Shang and Xu 2019). The results of the calculated electroosmotic permeability revealed the primitive ability of the electrokinetic process to facilitate water flow through the tailings.

Electric Current Variation

The amount of electric current directly depends on the resistivity of the tailings under the electrokinetic process, which is related to the water content, pH, and chemical interactions that occurred during the experiments. Increasing the resistivity during the electrokinetic water extraction process caused the electric current to drop to almost a constant value (Fig. 4a) and decreased the electromigration and electroosmosis potential. Moreover, in the electrokinetic studies, changing the electric current can affect the transport of ionic species and improve the electro-dewatering performance (Deng et al. 2020). The electric current intensity was frequently changed by reversing polarity in T2 and T3. Considering the trend of electric current, the T1 scenario showed a drop of electric current from above 200 mA to 40 mA during 48 h (2880 min), which then converged to 30–40 mA (Fig. 4a.).

The gradual drop of the electric current in the next 96 h of the T1 scenario led the slow physicochemical variation of the medium. The T2 scenario was conducted to investigate the effect of polarity reversal on the electric current variation besides the enhancement of water extraction and chemical reactions. The scheduling of polarity reversal was based on the electric current variation. When the electric current decreased and reached a constant value, the polarity was reversed. According to Fig. 4, in each polarity reversal, the current intensity increased to a maximum value and then decreased, reaching to a constant value over a period of ≈ 24 h. The polarity reversal of T2 and T3 scenarios started after 48 h and during the experiments, four series of polarity reversals were applied.

It is noteworthy that the polarity reversal series 1 and 3 illustrated a lower increase of current intensity than series 2 and 4. The possible reason is that the reversal of the anode–cathode position and production of regenerated acid–base buffer the acidic or basic condition in the anode and cathode. Consequently, the resistivity of the medium increases, leading to a smaller increase in current intensity. Comparing the electric energy consumption of T1 and T2 demonstrated that polarity reversal improved the electric current variation, but, according to Eq. 3, increased the

energy consumption of the system. Moreover, fewer voltage gradients in T3, caused less energy consumption and electric current use (Fig. 4b).

Moisture Content

At the end of the experiments, tailings samples were taken from different sections of the box to measure the moisture content. Figure 5 shows the moisture in all five sections in T1, T2, and T3. In general, an ascending trend of moisture content from the anode to the cathode was observed. The average moisture value was higher in T3 than in T1 and T2, due to less water reduction due to evaporation, heat generation, and hydrolysis around the electrodes in the T3 scenario. The moisture content of T1 and T2 were almost the same. However, T2 and T3 showed almost identical moisture content variations in the middle parts of the setup due to polarity reversal.

The total amount of removed water (the total amount of water extracted from the tailings and lost to evaporation and hydrolysis) were 7.6%, 7.7%, and 5.6%, for T1, T2, and T3, respectively. The extracted water in all of the experiments was also estimated at $\approx 5\%$ of the initial weight of the samples. Comparing the percentage of the extracted water and the amount of removed water from the experiments, it clear that the evaporation and hydrolysis phenomena were stronger in the T1 and T2 scenarios (Fig. 5).

The amounts of energy consumed to remove the unit weight of trapped water from the tailings were 1.28, 1.65, and 0.77 (kWh/kg-removed water) for T1, T2, and T3, respectively (Fig. 6). Previous work has indicated the values of 0.001 to 1.2 (kWh/kg-removed water) for removing water from mineral tailings with a variety of mineralogical compositions and water content (Dizon and Orazem 2020). Although T3 consumed the least amount of energy to remove the unit weight of water from the tailings, more water was removed in T1 and T2, and the moisture content was reduced to less than the liquid limit (25%, according to Table 1).

pH Variation of the Tailings

The pH variations for different sections of the experimental setup showed a nearly similar trend for all three experiments and scenarios (Fig. 7). The highest pH variations occurred at the anodes and cathodes. A pH drop was observed below the PZC near the anode in T1 and T2, which could have reduced the average electroosmotic permeability of the tailings. However, the overall pH of the tailings in each experiment was higher than PZC value and no reverse electroosmotic flow occurred within 144 h, due to the polarity reversal in T2 and T3 as well as the pH adjustments of the anode and the cathode sides.

Accordingly, the highest variations of pH were observed in experiment T1. Moreover, no specific variation was observed in the central parts of T1. Decreasing the production rate of H^+/OH^- and the effects of soil buffering prevented the spreading of acidic/alkaline fronts toward the central portion of the experimental set-ups. However, T2 was able to reduce the pH of the central parts by ≈ 1 unit during the 144 h.

Electrical Conductivity (EC) of the Pore Fluid

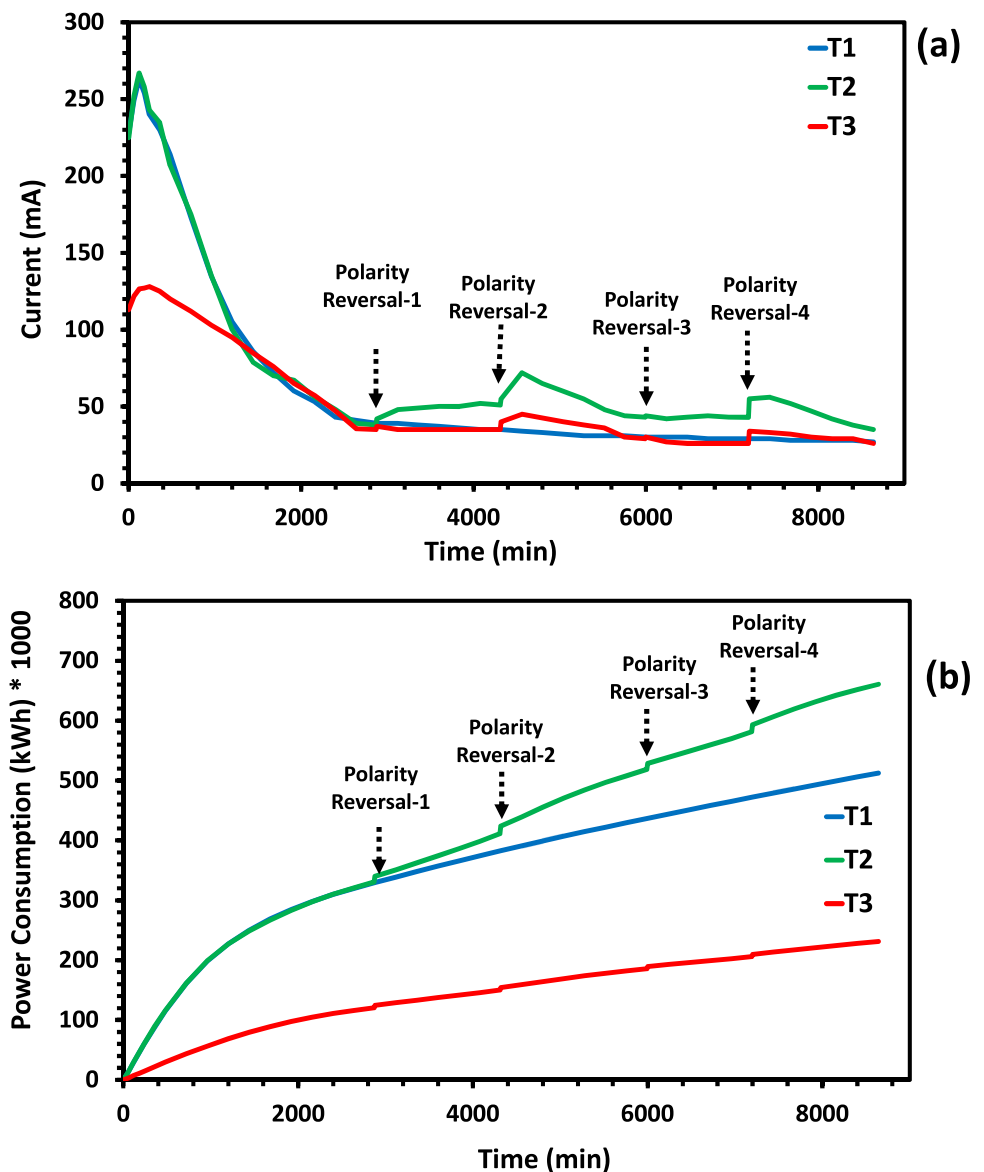
The EC is mainly related to the ionic composition of the tailings material. The initial EC was measured at ≈ 1.9 (mS). The EC values of the anode were higher than the values of the central and cathode parts (Fig. 7b). Due to electromigration, the EC values of the middle and cathode parts for all

of the experiments decreased from their initial values. The release of elements, especially potentially toxic metals, from the acid-soluble fraction to the exchangeable fraction, was the main cause of the EC increase near the anode.

Electrical Resistivity of the Tailings

The resistivity of the tailings is directly related to a sample's moisture and ionic concentrations. At the first stage of all of the experiments, both of these affected the resistivity of the media. The similarity between the resistivity profile trends and EC at 144 h indicated the further influence of the pore fluid's ionic composition on resistivity. During the electrokinetic process, the resistivity changed due to changes in the EC, ionic composition, and moisture content of the media. Nevertheless, the gradual variability of the moisture content

Fig. 4 **a** Electric current (mA) and **b** cumulative energy consumption (kWh) of each experiment. Polarity reversal periods for T2 and T3 are illustrated on the graphs



at the end of the experiments indicated that the moisture content had less of an effect on the resistivity of the tailings (Fig. 7c).

Electrokinetic Dewatering and Extracted Water

The extracted water was measured within 3–144 h. The electric current and collected water generally decreased after 48 h in T1. During this time, the maximum amount of extracted water (244 mL) was achieved and the electric current dropped to 30–40 mA (Fig. 4). T1 and T2 both showed the same trend on the amount of collected water within 48 h. By reversing polarity and modifying the electric current, T2 extracted 265 mL of water over 144 h. Moreover, applying a voltage gradient of 1 V/Cm with polarity reversal extracted a total amount of 250 mL of water in the T3 scenario with the least amount of energy consumption (Fig. 8).

The rate of extracted water decreased during the electrokinetic process due to the physicochemical variability of the tailings (Fig. 8b). The flow rate was measured as 22.6, 23, and 10.6 (mL/h) for T1, T2, and T3, respectively, in 3 h. The amount of extracted water for 3–144 h decreased during the experiments, causing the flow rate to drop to 1.68 (T1), 1.84 (T2), and 1.7 (T3). Reductions in the rate of collected water and electroosmotic flow has also been well documented by

previous researchers (Fourier and Jones 2010; Shang and Xu 2019).

It was expected that in a normal condition, the amount of electric current intensity and the extracted water of T1 and T2 would be twice as much as the T3 scenario. This condition was observed for the first 3 h of the experiments, since the effects of moisture and chemical changes on the tailings resistivity values were not significant (Fig. 8b). As time progressed, the amount of extracted water and electric current variations deviated from the expected condition due to the physicochemical effects. In fact, these effects were observed from 3 to 144 h. Accordingly, after 24 h, water extraction was approximately the same for T1, T2, and T3. Thus, the maximum potential of the experiments to extract the trapped water was achieved in 24 h.

To compare the amount of electric energy consumption and recovered water from the experiments, IDT, IWE and INWE were calculated (Fig. 9). The values of IDT were in the range of 6–600 (kWh/dry-ton), reported by Bourguès-Gastaud et al. (2017) and Fourie and Jones (2010). The values of IWE and INWE were both the same for the first 48 h of T1 and T2. In addition, the polarity reversal scenario increased energy consumption over the time as well as the values of the indices. Also, the T3 scenario consumed less energy due to the use of a lower voltage gradient. Consequently, T3 showed lower index values.

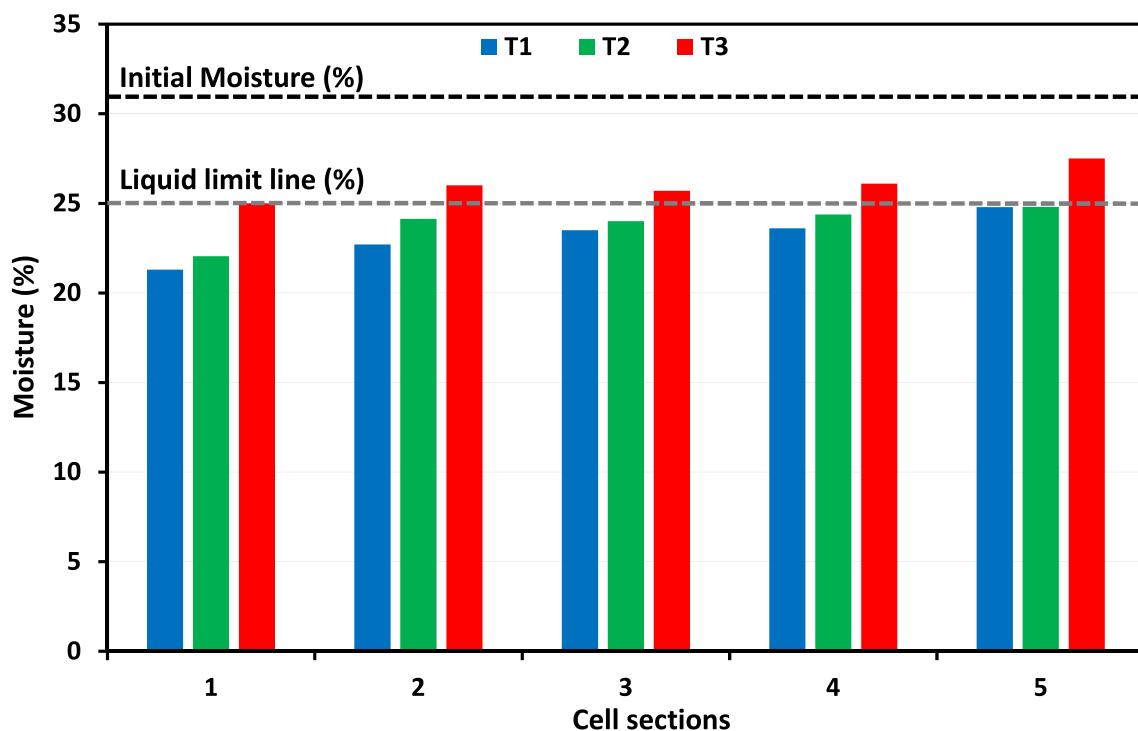


Fig. 5 Moisture variation of the tailings, initial moisture content and liquid limit of the tailings materials

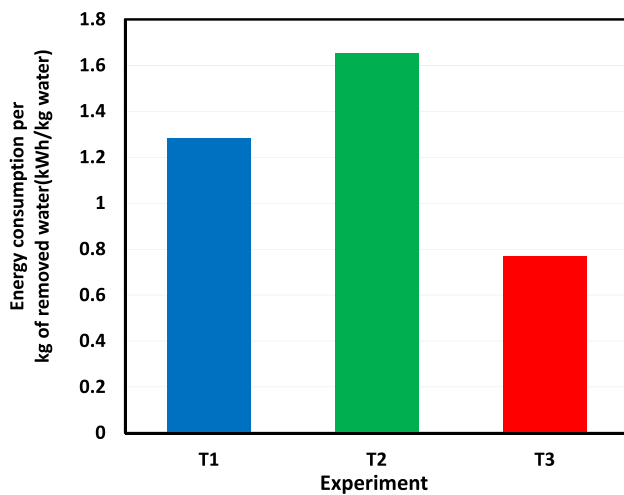


Fig. 6 Moisture reduction of the experiments by considering the energy consumption

Although the overall extracted water in T2 was higher than T1 and T3, it was not an optimal scenario based on the indices. According to Fig. 9, INWE and IWE were both optimal in the T3 scenario for the first 24 h. The minimum values of the IWE and INWE were calculated as 0.39 (kWh/L) and 72.95(kWh/dry-tonne·L), respectively. In this situation, the energy consumption of the experiment was 0.084 (kWh) and the extracted water was 214 mL. The optimal situation of T1 and T2 were also observed in the first 3 h of the experiments. Note that it is important to calculate the cost of electricity for extracting 1 mL of water from a certain amount of tailings and compare it with the required cost to extract this water by other technologies, to evaluate the optimal economic situation.

One of the main chemical parameter of the processing water is pH. It is important to monitor the acidity of the extracted water for reuse by the mining sectors and processing plant. The pH values are given in Table 3. The extracted water from the cathode side had pH values above 12 during the first 48 h of the experiments. Conversely, by reversing the poles during 48–72 h of T2 and T3, trapped water was extracted from the primary anode side with a pH of ≈ 3 . By applying a second polarity reversal between 72 and 96 h, the situation of electrodes returned to the primary position and the pH of the extracted water increased to 9.4 and 9.92 in T2 and T3, respectively. Based on the pH of the processing water in the Miduk copper mine, which is in the basic range, the results showed that the pH values of the water extracted during hours 3 and 24 were suitable for return to the processing plant.

The chemistry of the initial processing water and overall extracted water were also investigated by measuring the amount of potentially toxic metals by ICP-OES analysis (Table 4). In comparison to the processing water, the

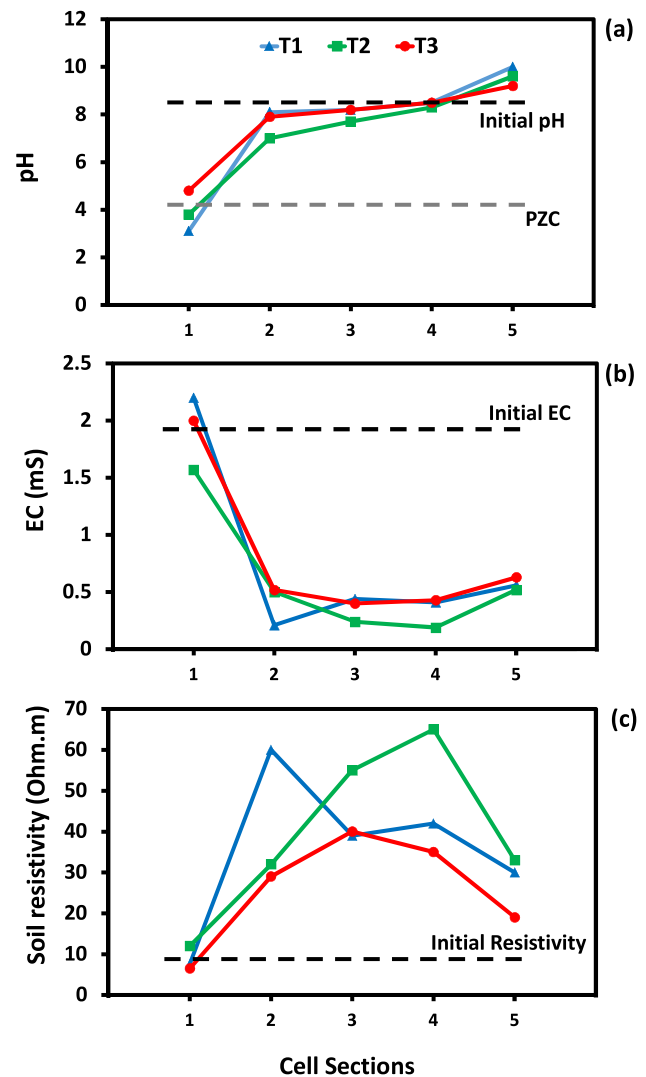


Fig. 7 Physicochemical variation of the tailings (pH, EC, resistivity) after the experiments compared to the initial values

amount of these elements of the final extracted water was not changed significantly, and was in the acceptable range for reuse by the processing plant. It is noteworthy that the formation of an unknown brown precipitate strongly affected the chemistry of the extracted water due to the probable precipitation and adsorption of the toxic elements. The reason of this process was the basic range of the pH values at the end of the experiments. The chemical composition of the precipitates was unclear due to the unanalyzable amounts of the products.

The Effect of Dewatering on the Chemical Composition of the Tailings

Mineralogical and chemical compositions of the tailings materials prior to and after the electrokinetic dewatering test

were performed by XRD analysis and sequential extraction. Comparison of the XRD analyses indicated that the major mineralogy was not influenced by the electrokinetic process, nor was acid–base production. As shown in Fig. 10, the major mineralogy of the samples from the anode and cathode sections of scenario T2 was not changed significantly in comparison with the initial mineralogy of the tailings.

Also, the sequential extraction procedure was performed for three fractions including exchangeable, acid-soluble and residual phases. Figure 11 shows the chemical analyses and different fractions of the representative sample of the intact tailings for potentially toxic elements. The highest total metal content was observed in the residual phase. The exchangeable fraction for the selected elements was less than 1% of the total amount.

The maximum ability of the electrokinetic dewatering process to release the elements from the media is equal to the sum of exchangeable and acid-soluble phases, which is

called the extractable fraction. About 20% (90 mg/L) of the copper was in the acid-soluble fraction (Fig. 11).

According to the higher concentration of copper, especially in the acid-soluble fraction, release and transport of this element was examined for each scenario (Fig. 12). Compared with the initial value, the maximum amount of exchangeable copper was observed at the anode sides of all the experiments. This increase at the anode represented copper released as a consequence of acid production, from the acid-soluble and exchangeable fractions. Also, the pH variations had a direct effect on the release of copper from the media.

The maximum value of the copper exchangeable fraction was observed in the T1 scenario (Fig. 12a). However, the transport process was limited due to the low electric current and moisture value. In the T2 scenario, the copper in the exchangeable fraction was lower than in the T1 scenario around the anode (Fig. 12b). This was due to copper removal as well as the transport process occurring

Fig. 8 Extracted water (a) and flow rate (b) of T1, T2 and T3

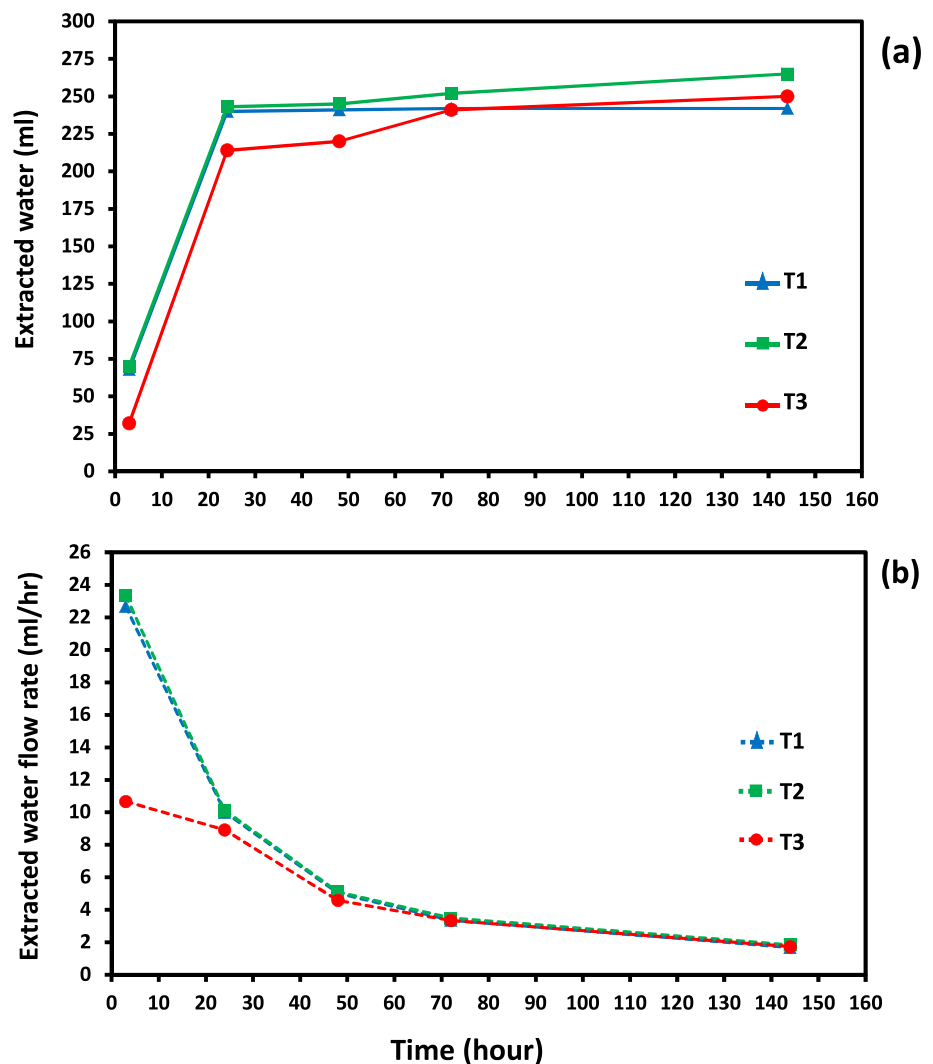
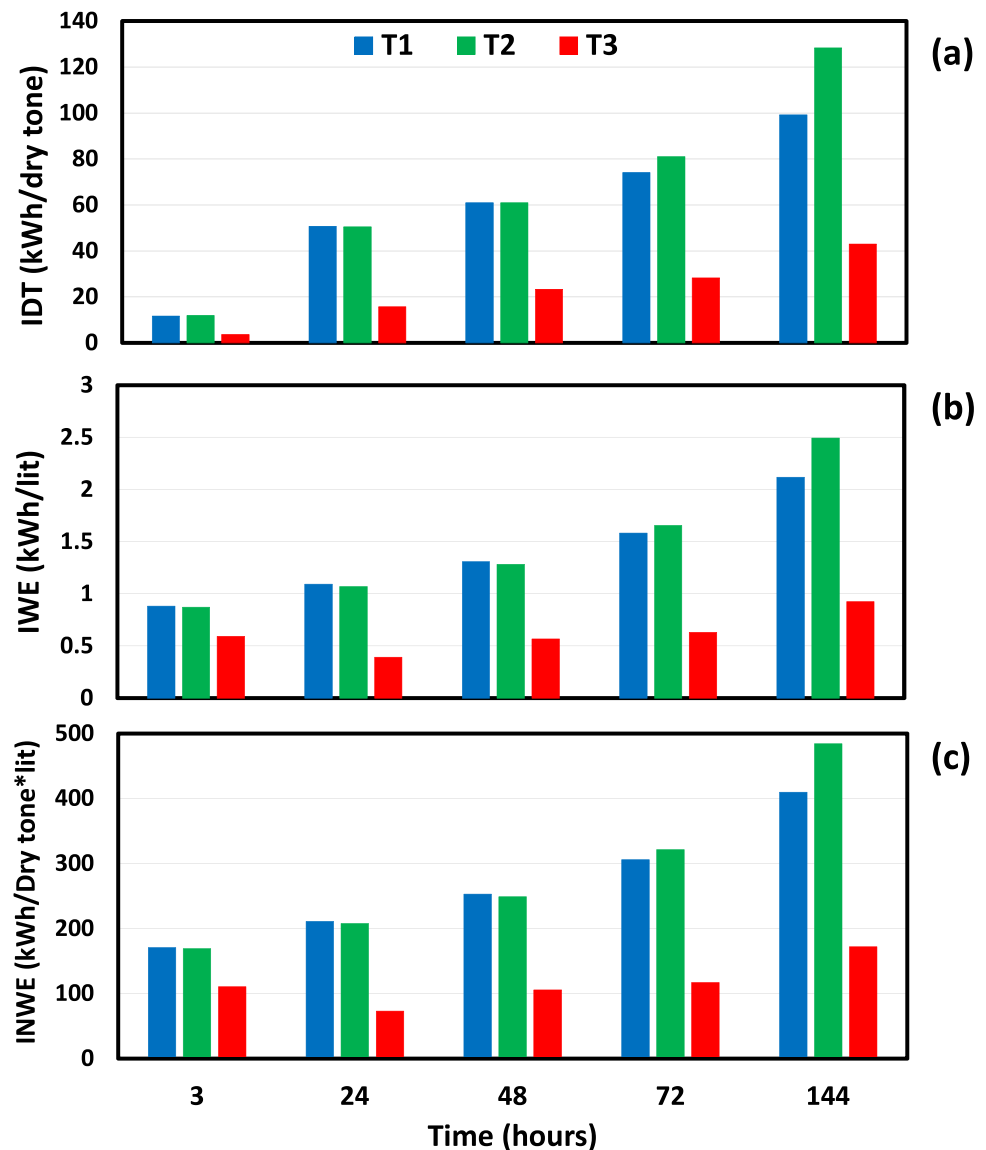


Fig. 9 Index of dry-tone (IDT), water extraction (IWE) and normal water extraction (INWE) to evaluate the energy consumption and system efficiency



toward the cathode side. Despite the polarity reversal in T2, an increase in the copper content of the exchangeable fraction in Sect. 2 of the cell revealed that copper was being transported toward the cathode side. Figure 12c illustrated that in the T3 scenario, the amount of removed copper and exchangeable phases were less than in T2 and T1, respectively.

In addition, T2 was able to reduce the initial copper content by 6% of the total and 34% of the extractable fractions, respectively, at the anode (Fig. 12d) due, at least in part, to the copper extraction and transport that occurred during polarity reversal. As shown in Fig. 12d, copper removal in T3 was $\approx 2.5\%$ of the total and 13% of the extractable values near the anode.

Results indicated that dewatering process affected the release and transport of copper due to the reduction of

electric current and pH changes. Moreover, decreasing the moisture content could change the degree of saturation and decrease the transport process of the elements as well as the resistivity variation. Overall, the electrokinetic process for copper removal from the tailings was not significant and only observed near the anodes of all the experiments. The reasons for this include short experimental duration, acid-buffering of the tailings, and H^+ neutralisation. Also,

Table 3 pH variation of extracted water in different scenarios

Experiment ID	pH-3 h	pH-24 h	pH- 48 h	pH-72 h	pH- 96 h
T1	12.2	12.5	12.5	–	–
T2	12.2	12.5	12.6	3	9.4
T3	12.4	12.4	12.5	3.6	9.92

Table 4 Chemical analysis of extracted and processing water for toxic elements in mg/l

Elements	Sample ID			Processing water of Miduk copper mine	Fisheries an aquatic water ^a (Chapman 1996)
	T1	T2	T3		
Chemical Analysis in mg/l					
Al	0.1	6.7	5.3	0.7	0.1
As	<0.05	<0.05	<0.05	<0.05	0.05
Cd	<0.05	<0.05	<0.05	<0.05	0.005
Co	<0.05	<0.05	<0.05	<0.05	0.01
Cr	0.5	0.5	0.4	<0.05	0.02
Cu	0.14	0.2	0.14	0.1	0.002
Fe	1.5	0.5	0.6	0.2	0.3
Mg	1.4	0.4	0.4	6	–
Mn	<0.1	<0.1	<0.1	<0.1	–
Mo	0.1	0.8	0.2	0.1	–
Ni	<0.05	<0.05	<0.05	<0.05	0.025–0.15
Pb	<0.05	<0.05	<0.05	<0.05	0.001
V	<0.05	<0.05	<0.05	<0.05	–
Zn	<0.05	<0.05	<0.05	<0.05	0.03

^aCanadian Water Quality Guidelines, 1987

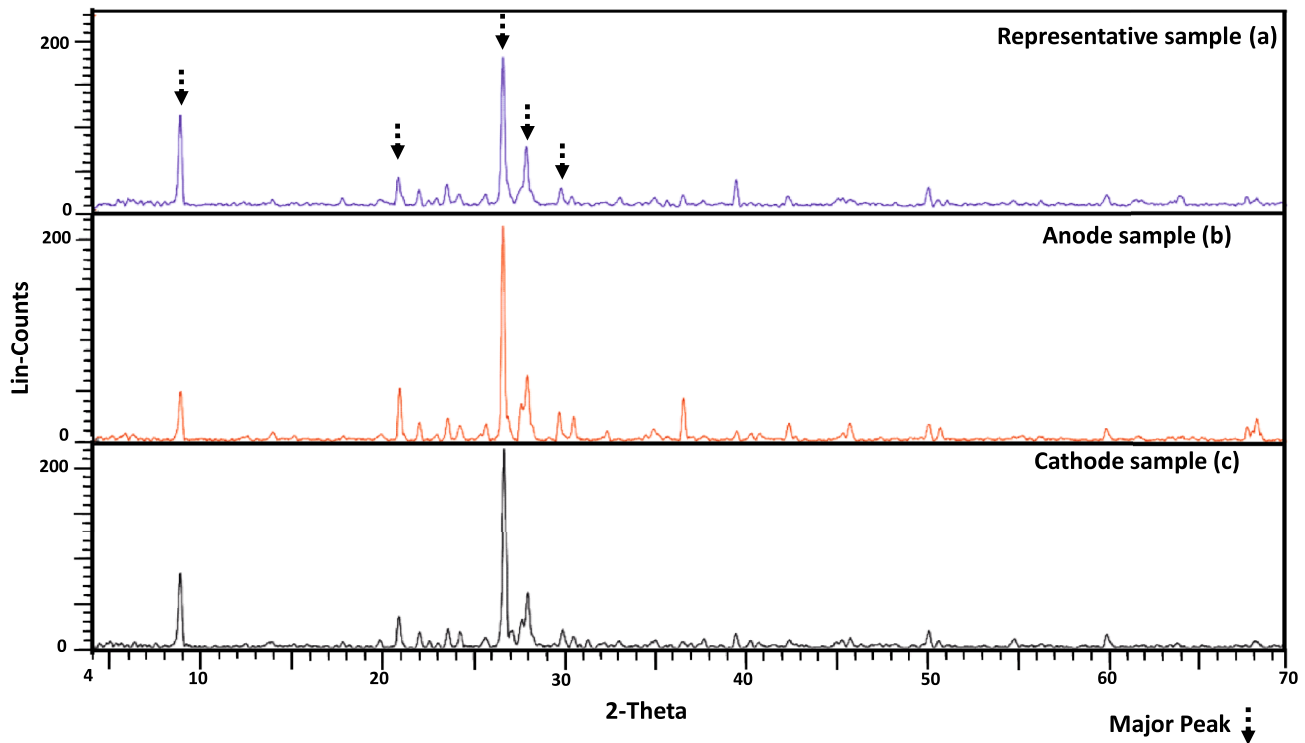


Fig. 10 Mineralogical analysis of the representative tailings sample (upper) compared to anode (middle) and cathode (lower) sections of experiment T2

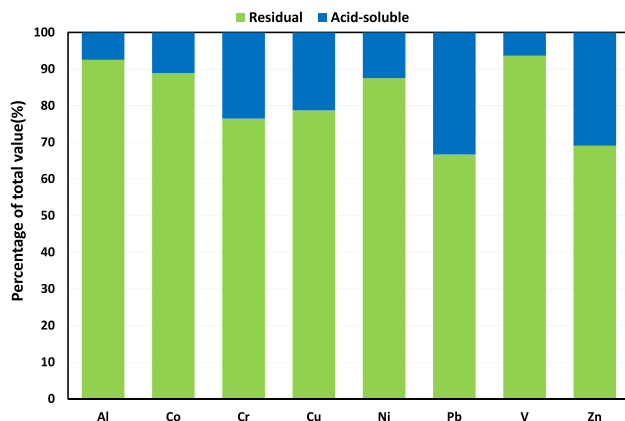


Fig. 11 Residual and acid-soluble fractions as a percentage of total metal content

moisture reduction decreased the rate of hydrolysis of the media and reduced the potential of electrokinetics to release and transport the copper.

Electrokinetic Dewatering in Practice

The main costs of pilot-scale electrokinetics are related to the energy consumption and electrode type. Practical implementation of electrokinetic process in a pilot scale is also

very complex. However, laboratory tests give us some valuable information about the technical feasibility of an electrokinetic process (López-Vizcaíno et al. 2019).

Based on the experimental results, T2 recovered the greatest amount of trapped water from the tailings. Considering the moisture variation, T1 and T2 reduced the moisture content of the tailings to less than the liquid limit of the materials (25%). However, by considering the amount of energy consumption, scenario T3 represented the least amount of energy consumption to extract trapped water within 24 h.

By considering chemical variations, T2 showed the most copper removal at the anode. However, the maximum amount of the exchangeable copper was observed in the T1 scenario due to less electromigration and release and transport of copper from within the tailings. Since increasing the amount of remained exchangeable copper through the tailings medium increases the environmental risk of the tailings over the time, reversing polarity can weaken the environmental risks of electrokinetic dewatering. By reversing polarity, suitable amounts of copper, as well as the exchangeable fraction near the anode, can be removed from the tailings medium.

The highest corrosion rate of the electrode (5.2% of the initial weight) was observed in T1. Scenarios T2 and T3 had corrosion rates of $\approx 4.3\%$ and 3.9% , respectively in

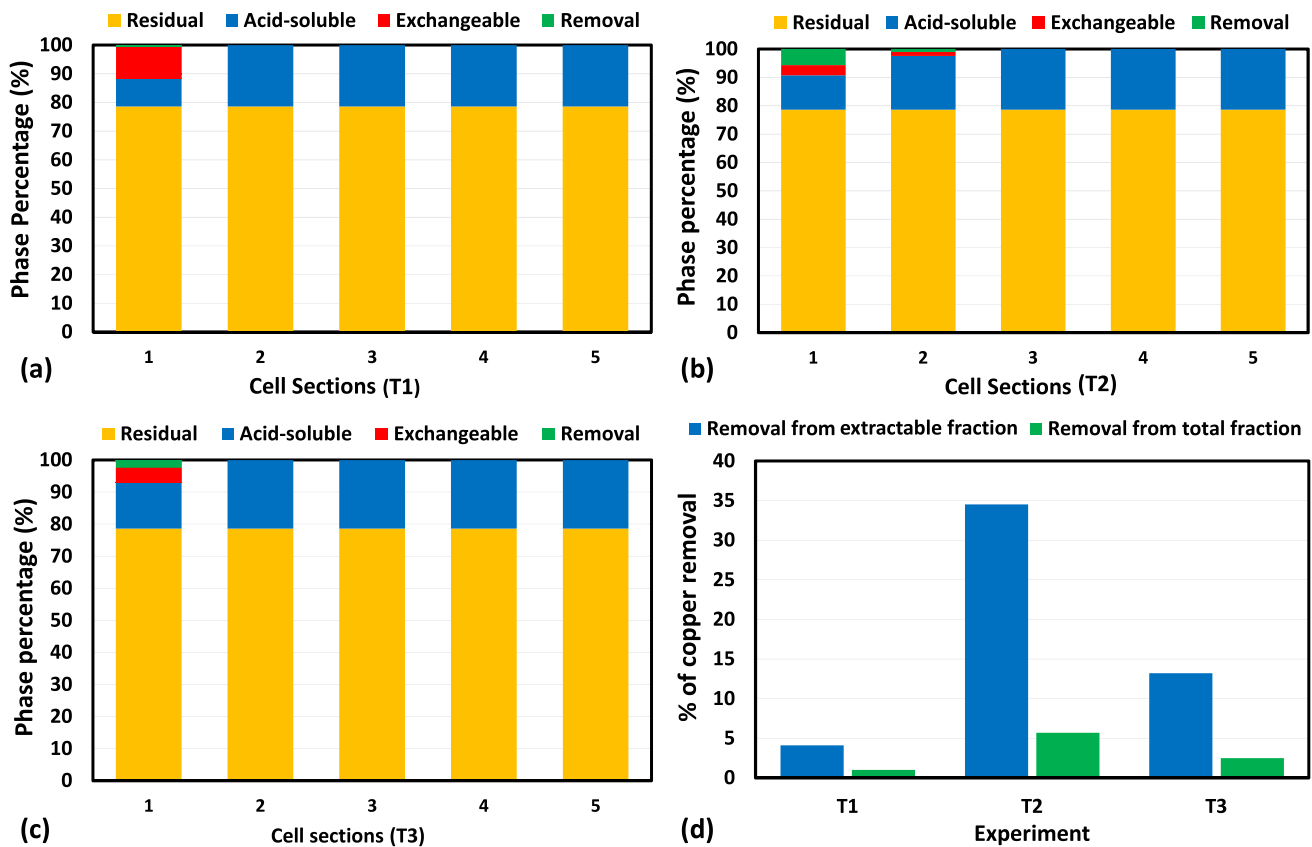


Fig. 12 Copper percentages in different fractions of three scenarios in various cell section (a, b, c), and copper removed from the extractable and total fractions around the anode side (d)

the experimental condition. Accordingly, polarity reversal reduced the electrode corrosion rate of SS316 electrodes in the pilot-scale scenarios.

Generally, in the case of water extraction in a pilot-scale application, a voltage gradient of 1 V/cm and polarity reversal are recommended to extract more trapped water from within the tailings. To optimize the energy consumption, dividing an area into grids of 1 m × 1 m or 2 m × 2 m and a depth of 1–2 m is recommended. Higher grid size increases the voltage levels and electric energy consumption. Electric potentials of 100–200 V are also needed to apply a voltage gradient of 1 V/cm. The environmental impact of the process can also be reduced by applying a voltage gradient of 1 V/cm.

Measuring the resistivity of the tailings sample was indicative of the effects of electrokinetic process on the moisture and chemical variation. So, in pilot-scale applications, monitoring the process using geo-electrical methods will aid in estimating the moisture content and optimizing the duration of the process.

Summary and Conclusion

Electrokinetic dewatering is a suitable method to extract trapped water from mine tailings. Moreover, the efficiency of water extraction and electric energy consumption was evaluated using three indices implementing three experimental scenarios. Also, the effect of dewatering on the physico-chemical variation and copper removal in tailings materials were investigated by applying a sequential extraction procedure. Among the three implemented scenarios, the highest extracted water was associated with scenario T2, with polarity reversal and 2 V/cm voltage gradient. The highest moisture reduction was also observed in T1 and T2 due to the effects of hydrolysis of water molecules around the electrodes and heat production. However, the IWE and INWE indices showed the best energy consumption belonged to the first 24 h of the T3 experiment. In addition, the corrosion rate of the electrode was lowest in T3. The final pH values of the anode and cathode parts were ≈ 4 and 10, respectively. Considering the PZC of the tailings, these pH values were not in the range of reverse electroosmotic flow.

To evaluate the mass transport phenomenon, the extracted copper was defined as the copper removed from

the acid-soluble fraction and totalled 34% on the anode side of T2. This scenario indicated the best copper removal, due to the higher electric current and polarity reversal. The EC values of the pore water and the resistivity of the tailings showed a reasonable accordance in the anode parts of T1, T2, and T3, and this was also confirmed by the sequential extraction results. High voltage gradients had a direct influence on the reduction of moisture content as well as the release and removal of chemical components by hydrolysis and electromigration processes. It also decreased the efficiency of water extraction. Considering the electric energy consumption and the efficiency of water extraction, T3 is the most favourable scenario to recover the trapped water from the tailings due to the low voltage gradient and polarity reversal. It also released the least amount of contaminant from the corroded electrode to the tailings media. Applying polarity reversal decreased the exchangeable fraction of copper as an environmental mobile phase near the anode side. The dewatering process also reduced the effect of hydrolysis and electromigration on copper remediation. It seems that increasing the duration of the experiments will not significantly affect the efficiency of the remediation process due to moisture content reduction. The media resistivity was affected the voltage and electric current drop, which influenced the electrokinetic performance. So monitoring the resistivity with fixed corrosion-resistant electrodes will help investigate moisture content and chemical changes. Finally, a combination of polarity reversal with the injection and circulation of acidic reagents around the electrodes is suggested to maximise the electroosmotic and electromigration processes, especially for pilot scale or in-situ field applications.

Acknowledgements This article is part of a research project focused on monitoring and modelling of the electrokinetic process on the dewatering and remediation of mine tailings at the Miduk copper mine in Kerman, Iran. The authors are grateful to the R&D Division of the National Iranian Copper Company (NICICO) for their cooperation. The authors also thank Dr. S Maghsoudy, Mr. MJ. Khakpour, Mr. H. Mousavi, Mrs. R. Siyar, and Mrs. S.S. Saadaatmir for their technical and experimental support.

References

- Abdullah W, Al-Abadi A (2010) Cationic–electrokinetic improvement of an expansive soil. *Appl Clay Sci* 47:343–350. <https://doi.org/10.1016/j.clay.2009.11.046>
- Acar YB, Alshawabkeh AN (1993) Principles of electrokinetic remediation. *Environ Sci Technol* 27:2638–2647. <https://doi.org/10.1021/es00049a002>
- Ammami M, Song Y, Benamar A, Portet-Koltalo F, Wang H (2020) Electro-dewatering of dredged sediments by combined effects of mechanical and electrical processes: Influence of operating conditions. *Electrochim Acta*. <https://doi.org/10.1016/j.electacta.2020.136462>
- Bourgès-Gastaud S, Dolez P, Blond E, Touze-Foltz N (2017) Dewatering of oil sands tailings with an electrokinetic geocomposite. *Miner Eng* 100:177–186. <https://doi.org/10.1016/j.mineng.2016.11.002>
- Cardenas-Peña AM, Ibanez JG, Vasquez-Medrano R (2012) Determination of the point of zero charge for electrocoagulation precipitates from an iron anode. *Int J Electrochem Sci* 7:6142–6153
- Chapman DV (1996) Water quality assessments: a guide to the use of biota, sediments and water in environmental monitoring. CRC Press, New York
- Chien S-C, Ou C-Y, Wang M-K (2009) Injection of saline solutions to improve the electro-osmotic pressure and consolidation of foundation soil. *Appl Clay Sci* 44:218–224. <https://doi.org/10.1016/j.clay.2009.02.006>
- Conrardy J-B, Vaxelaire J, Olivier J (2016) Electro-dewatering of activated sludge: electrical resistance analysis. *Water Res* 100:194–200. <https://doi.org/10.1016/j.watres.2016.05.033>
- Deng W, Lai Z, Hu M, Han X, Su Y (2020) Effects of frequency and duty cycle of pulsating direct current on the electro-dewatering performance of sewage sludge. *Chemosphere* 243:125372. <https://doi.org/10.1016/j.chemosphere.2019.125372>
- Dizon A, Orazem ME (2020) Advances and challenges of electrokinetic dewatering of clays and soils. *Curr Opin Electrochem* 22:17–24. <https://doi.org/10.1016/j.coelec.2020.03.002>
- Estabragh A, Naseh M, Javadi A (2014) Improvement of clay soil by electro-osmosis technique. *Appl Clay Sci* 95:32–36. <https://doi.org/10.1016/j.clay.2014.03.019>
- Fourie A, Jones C (2010) Improved estimates of power consumption during dewatering of mine tailings using electrokinetic geosynthetics (EKGs). *Geotext Geomembr* 28:181–190. <https://doi.org/10.1016/j.geotextmem.2009.10.007>
- Fourie A, Johns D, Jones CF (2007) Dewatering of mine tailings using electrokinetic geosynthetics. *Can Geotech J* 44:160–172. <https://doi.org/10.1139/t06-112>
- Guo Y, Shang JQ (2014) A study on electrokinetic dewatering of oil sands tailings. *Environ Geotech* 1:121–134. <https://doi.org/10.1680/envgeo.13.00013>
- Hansen HK, Rojo A (2007) Testing pulsed electric fields in electroremediation of copper mine tailings. *Electrochim Acta* 52:3399–3405. <https://doi.org/10.1016/j.electacta.2006.07.064>
- Huazhe J, Shufei W, Yixuan Y, Xinming C (2020) Water recovery improvement by shearing of gravity-thickened tailings for cemented paste backfill. *J Cleaner Prod* 245:118882. <https://doi.org/10.1016/j.jclepro.2019.118882>
- Karaca O, Cameselle C, Reddy KR (2017) Acid pond sediment and mine tailings contaminated with metals: physicochemical characterization and electrokinetic remediation. *Environ Earth Sci* 76:408. <https://doi.org/10.1007/s12665-017-6736-0>
- Kargar M, Khorasani N, Karami M, Rafiee G, Naseh R (2012) Statistical source identification of major and trace elements in groundwater downward the tailings dam of Miduk Copper Complex, Kerman. *Iran Environ Monit Assess* 184:6173–6185. <https://doi.org/10.1007/s10661-011-2411-1>
- Kossoff D, Dubbin W, Alfredsson M, Edwards S, Macklin M, Hudson-Edwards KA (2014) Mine tailings dams: characteristics, failure, environmental impacts, and remediation. *Appl Geochem* 51:229–245. <https://doi.org/10.1016/j.apgeochem.2014.09.010>
- Lee JK, Shang JQ, Xu Y (2016) Electrokinetic dewatering of mine tailings using DSA electrodes. *Int J Electrochem Sci* 11:4149–4160. <https://doi.org/10.20964/1009160>
- Lockhart N (1983) Electro-osmotic dewatering of fine tailings from mineral processing. *Int J Miner Process* 10:131–140. [https://doi.org/10.1016/0301-7516\(83\)90038-8](https://doi.org/10.1016/0301-7516(83)90038-8)
- López-Vizcaíno R, Yustres A, Sáez C, Cañizares P, Asensio L, Navarro V, Rodrigo M (2019) Techno-economic analysis of the scale-up process of electrochemically-assisted soil remediation. *J Environ*

- Manage 231:570–575. <https://doi.org/10.1016/j.jenvman.2018.10.084>
- Maghsoudy S, Ardejani FD, Molson J, Amini M, Ebrahimi L (2019) Application of geo-electrical tomography in coupled hydro-mechanical–chemical investigations in heap leaching. *Mine Water Environ* 38:197–212. <https://doi.org/10.1007/s10230-018-0557-6>
- Mahmoud A, Olivier J, Vaxelaire J, Hoadley AF (2010) Electrical field: a historical review of its application and contributions in wastewater sludge dewatering. *Water Res* 44:2381–2407. <https://doi.org/10.1016/j.watres.2010.01.033>
- Mahmoud A, Hoadley AF, Conrardy J-B, Olivier J, Vaxelaire J (2016) Influence of process operating parameters on dryness level and energy saving during wastewater sludge electro-dewatering. *Water Res* 103:109–123. <https://doi.org/10.1016/j.watres.2016.07.016>
- Maiz I, Esnaola MV, Millan E (1997) Evaluation of heavy metal availability in contaminated soils by a short sequential extraction procedure. *Sci Total Environ* 206:107–115. [https://doi.org/10.1016/S0048-9697\(97\)80002-2](https://doi.org/10.1016/S0048-9697(97)80002-2)
- Malekzadeh M, Lovisa J, Sivakugan N (2016) An overview of electrokinetic consolidation of soils. *Geotech Geol Eng* 34:759–776. <https://doi.org/10.1007/s10706-016-0002-1>
- Masi M, Ceccarini A, Iannelli R (2017a) Model-based optimization of field-scale electrokinetic treatment of dredged sediments. *Chem Eng J* 328:87–97. <https://doi.org/10.1016/j.cej.2017.07.004>
- Masi M, Ceccarini A, Iannelli R (2017b) Multispecies reactive transport modelling of electrokinetic remediation of harbour sediments. *J Hazard Mater* 326:187–196. <https://doi.org/10.1016/j.jhazmat.2016.12.032>
- Navab-Daneshmand T, RI B, Hill RJ, Frigon D (2015) Impact of joule heating and pH on biosolids electro-dewatering. *Environ Sci Technol* 49:5417–5424. <https://doi.org/10.1021/es5048254>
- Ortiz-Soto R, Leal D, Gutierrez C, Aracena A, Rojo A, Hansen HK (2019) Electrokinetic remediation of manganese and zinc in copper mine tailings. *J Hazard Mater* 365:905–911. <https://doi.org/10.1016/j.jhazmat.2018.11.048>
- Ou C-Y, Chien S-C, Wang Y-G (2009) On the enhancement of electroosmotic soil improvement by the injection of saline solutions. *Appl Clay Sci* 44:130–136. <https://doi.org/10.1016/j.clay.2008.12.014>
- Reddy KR, Cameselle C (2009) Electrochemical remediation technologies for polluted soils, sediments and groundwater. Wiley, Hoboken
- Rezaee M, Asadollahfardi G, Gomez-Lahoz C, Villen-Guzman M, Paz-Garcia JM (2019) Modeling of electrokinetic remediation of Cd- and Pb-contaminated kaolinite. *J Hazard Mater* 366:630–635. <https://doi.org/10.1016/j.jhazmat.2018.12.034>
- Rosestolato D, Bagatin R, Ferro S (2015) Electrokinetic remediation of soils polluted by heavy metals (mercury in particular). *Chem Eng J* 264:16–23. <https://doi.org/10.1016/j.cej.2014.11.074>
- Shang JQ, Xu Y (2019) Electrokinetic dewatering of mine tailings from hydrometallurgical processes. In: *Proc, 22nd International Conf on Paste, Thickened and Filtered Tailings*, Australian Centre for Geomechanics, pp 275–283. https://doi.org/10.36487/ACG_rep/1910_18_Shang
- Siyar R, Ardejani FD, Farahbakhsh M, Norouzi P, Yavarzadeh M, Maghsoudy S (2020) Potential of Vetiver grass for the phytoremediation of a real multi-contaminated soil, assisted by electrokinetic. *Chemosphere* 246:125802. <https://doi.org/10.1016/j.chemosphere.2019.125802>
- Wang C, Harbottle D, Liu Q, Xu Z (2014) Current state of fine mineral tailings treatment: a critical review on theory and practice. *Miner Eng* 58:113–131. <https://doi.org/10.1016/j.mineng.2014.01.018>
- Wu P, Pi K, Shi Y, Li P, Wang Z, Zhang H, Liu D, Gerson AR (2020) Dewaterability and energy consumption model construction by comparison of electro-dewatering for industry sludges and river sediments. *Environ Res*. <https://doi.org/10.1016/j.envres.2020.109335>
- Xue Z, Tang X, Yang Q, Tian Z, Zhang Y (2019) Influence of salt content on clay electro-dewatering with copper and stainless steel anodes. *Drying Technol* 37:2005–2019. <https://doi.org/10.1080/07373937.2018.1555709>
- Zhang L, Hu L (2019) Laboratory tests of electro-osmotic consolidation combined with vacuum preloading on kaolinite using electrokinetic geosynthetics. *Geotext Geomembr* 47:166–176. <https://doi.org/10.1016/j.geotextmem.2018.12.010>
- Zhang S, Yang Z, Lv X, Zhi S, Wang Y, Li Q, Zhang K (2017) Novel electro-dewatering system for activated sludge biosolids in bench-scale, pilot-scale and industrial-scale applications. *Chem Eng Res Des* 121:44–56. <https://doi.org/10.1016/j.cherd.2017.02.035>
- Zimmerman AJ, Weindorf DC (2010) Heavy metal and trace metal analysis in soil by sequential extraction: a review of procedures. *Int J Anal Chem*. <https://doi.org/10.1155/2010/387803>